Supporting Information

Citric acid-modulated carbon dots derived from black tea waste for multifunctional food packaging: anti-counterfeiting and UV-protective preservation

Yulu Liu [a], Jiamin Li [a], Yizhou Xiao [b], Yuchi Chen [a], Yunkai Zhou [a], Fangmei Zhou [a], Bingqi Zhu [a], Wenxiao jiang [c], Xing Chen [b], Guangming Li [a, *]

[a] School of Medical Technology and Information Engineering, Zhejiang Chinese Medical University, Hangzhou, Zhejiang 310053, China

[b] State Key Laboratory of Food Science and Resources, College of Food Science & Technology, Nanchang University, Nanchang, Jiangxi 330047, China

[c] Department of Nutrition and Food Hygiene, School of Public Health, Shenzhen University Medical School, Shenzhen University, Shenzhen 518055, China Nanchang, Jiangxi 330047, China

* Contact information:
Guangming Li (GML), Tel: +86 15948350475; Fax: N/A; Address: School of Medical Technology and Information Engineering, Zhejiang Chinese Medical University, Hangzhou, Zhejiang 310053, China
E-mail: guangmingli2020@163.com

Supporting Figures

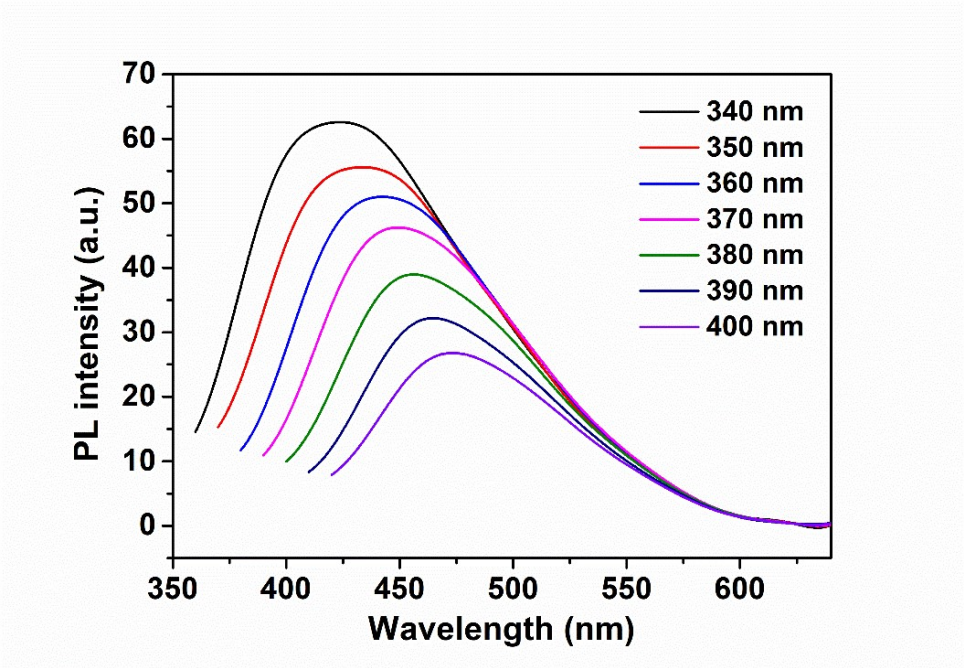

Figure S1. Fluorescence emission spectra of CDs derived from urea and black tea.

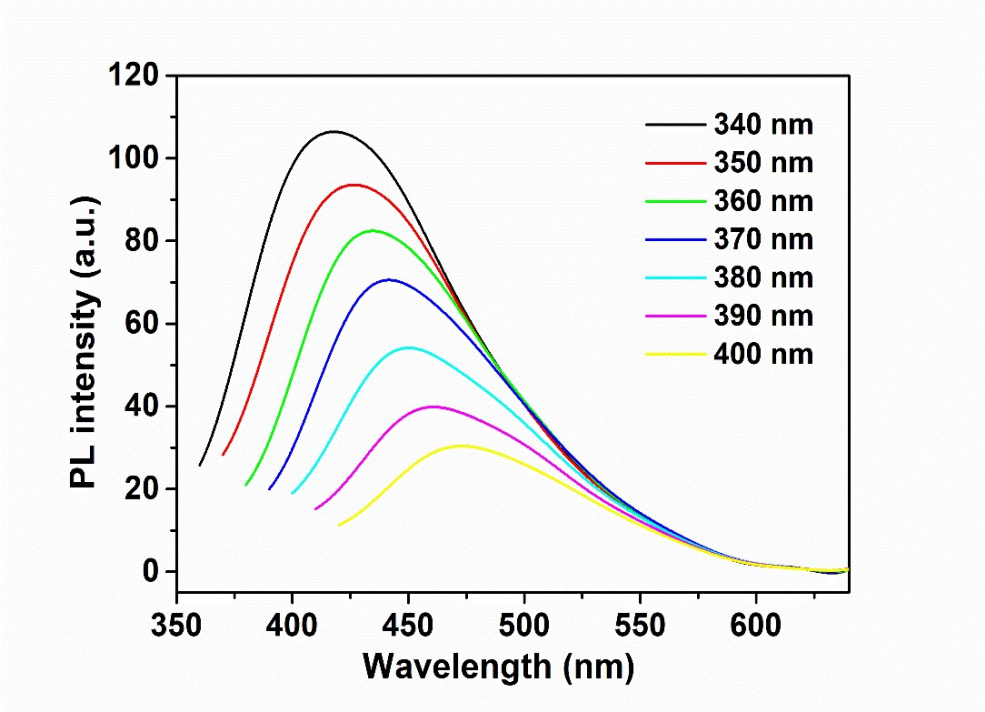

Figure S2. Fluorescence emission spectra of CDs prepared from melamine and black tea.

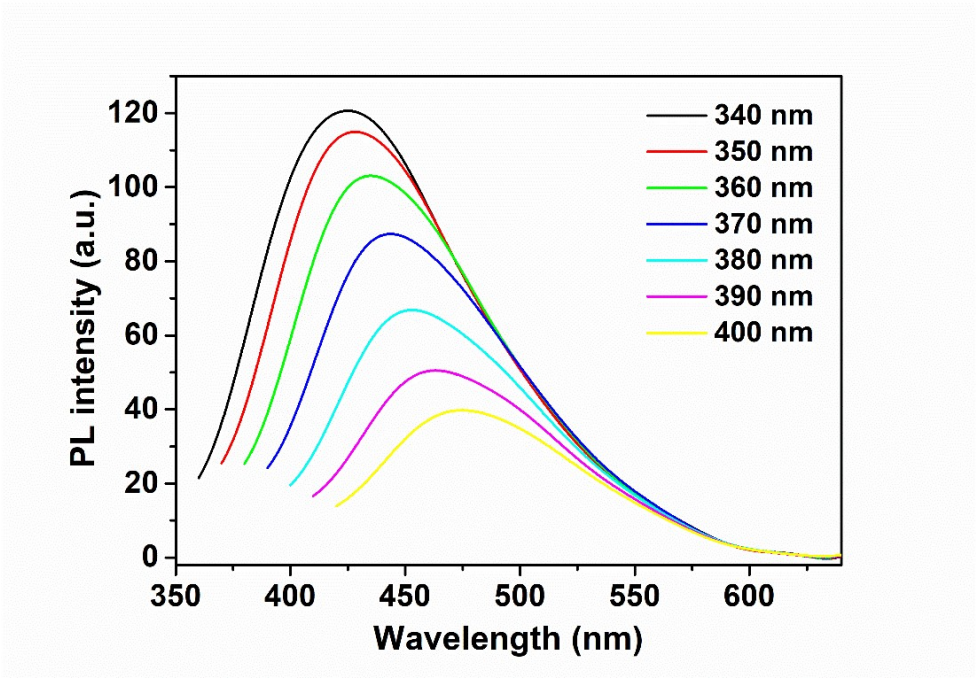

Figure S3. Fluorescence emission spectra of CDs prepared from arginine and black tea.

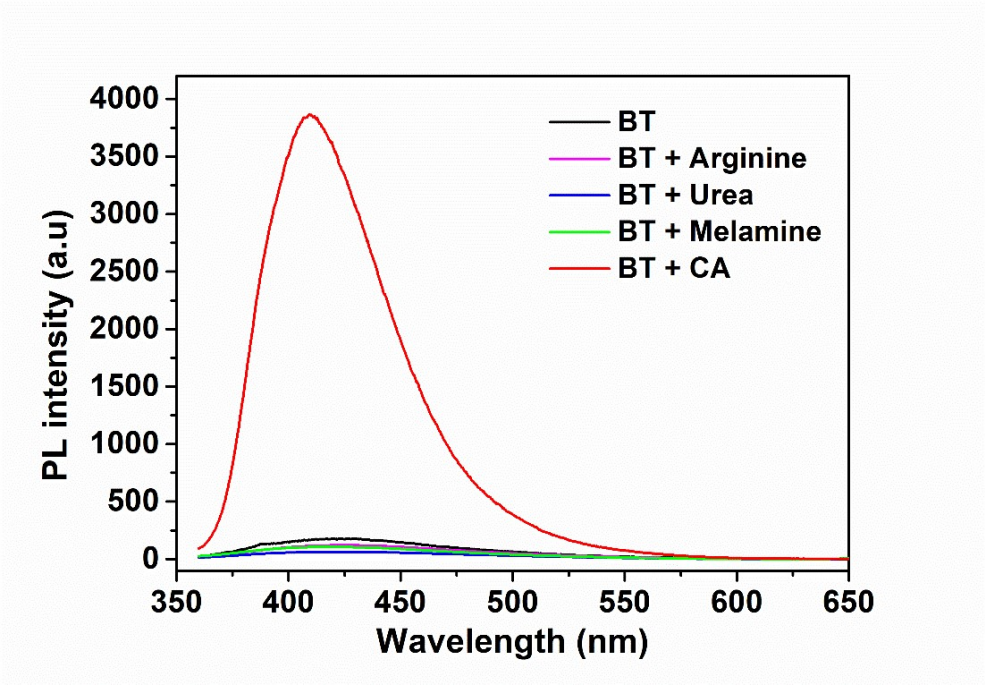

Figure S4. Fluorescence emission spectra (λ_{ex} = 340 nm) of CDs derived from black tea waste alone and with various additives (arginine, urea, melamine, and citric acid). Both the fluorescence intensity and the emission peak position exhibit a strong dependence on the additive used, with citric acid yielding the highest intensity.

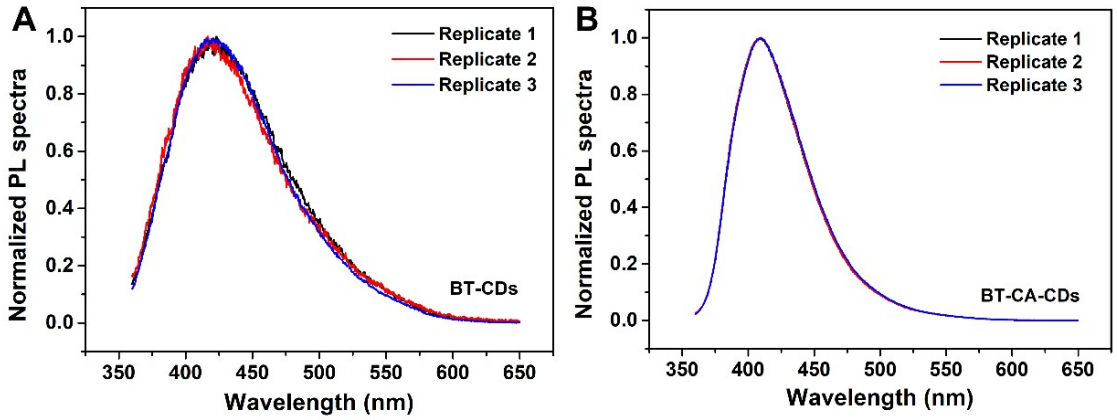

Figure S5 Fluorescence emission spectra of two CDs under 340 nm excitation, obtained from three independent synthetic replicates. The spectra exhibit excellent reproducibility, with both peak shape and peak position remaining consistent across all replicates.

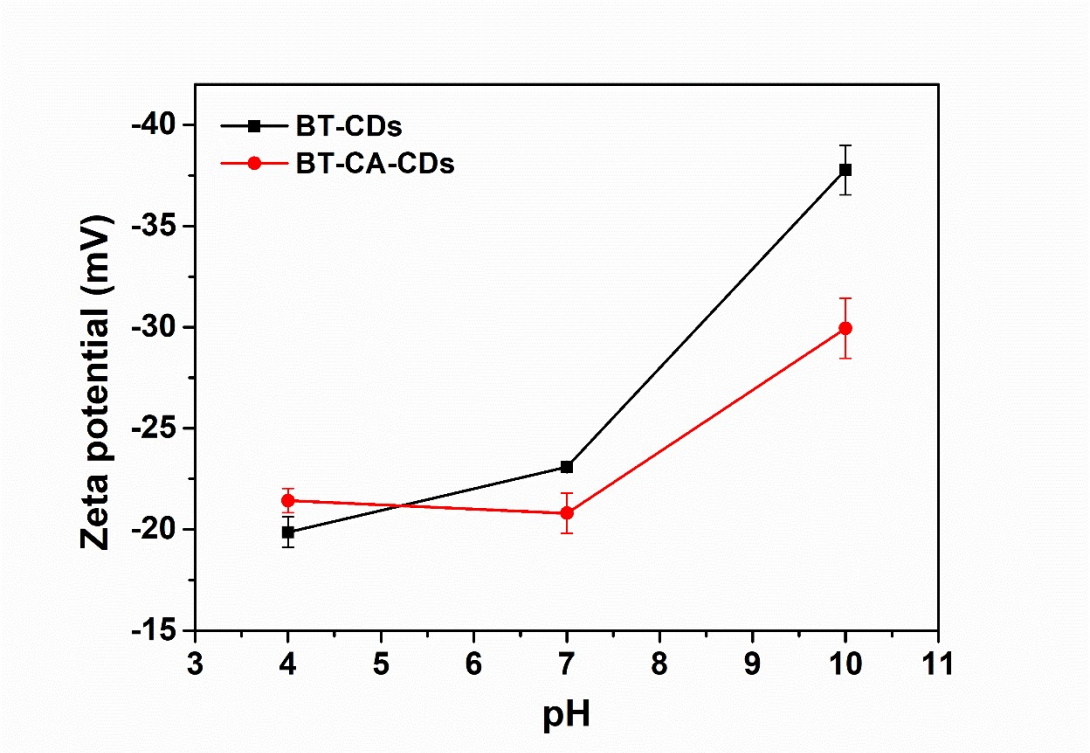

Figure S6. The zeta potential of BT-CDs and BT-CA-CDs varied with pH in the range of 4 to 10. Both CDs exhibit negative surface charges across all tested pH values. BT-CDs show a sharp negative shift at pH 10, while BT-CA-CDs display a milder pH response with a less negative value, indicating the formation of a dense passivation layer on the surface of BT-CA-CDs (n=3).

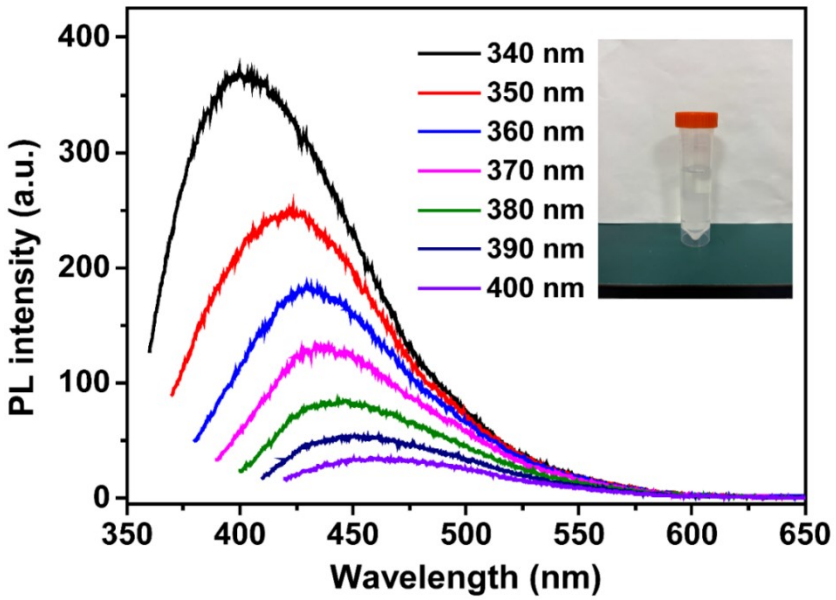

Figure S7. Fluorescence emission spectra of the crude sample prepared using citric acid alone as the raw material under excitation at different wavelengths. The spectra show negligible fluorescence emission, indicating that citric acid alone does not produce strongly fluorescent carbon dots under the same hydrothermal conditions.

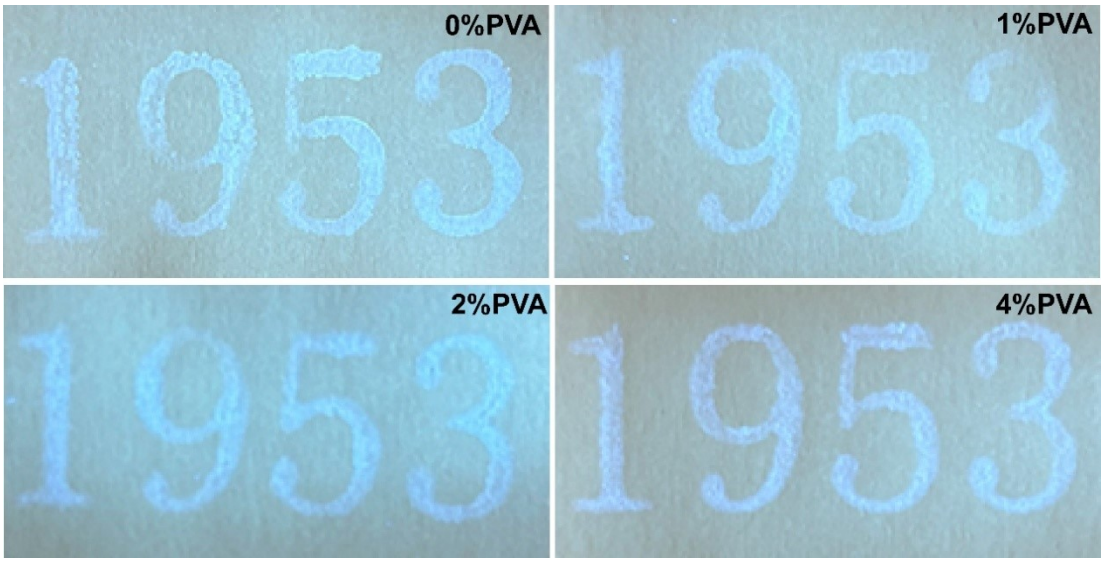

Figure S8. Digital image of stamp impressions fabricated from mixtures of BT-CA-CDs with different concentrations of PVA (0, 1, 2 and 4 wt%), captured under 365 nm UV illumination. The uniformity of the stamp impressions varies with PVA concentration, with optimal performance observed at 4 wt% PVA.

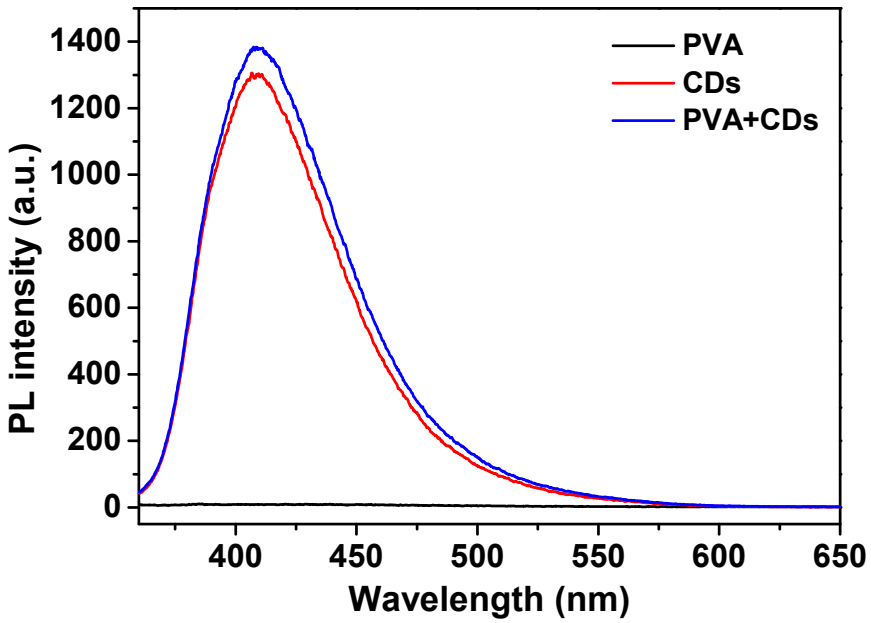

Figure S9. Fluorescence spectra of pure PVA, BT-CA-CDs alone, and the BT-CA-CDs/PVA composite. The spectra demonstrate that PVA itself exhibits negligible fluorescence, while the composite preserves the characteristic emission of the CDs, indicating no significant fluorescence change upon incorporation into the PVA matrix.

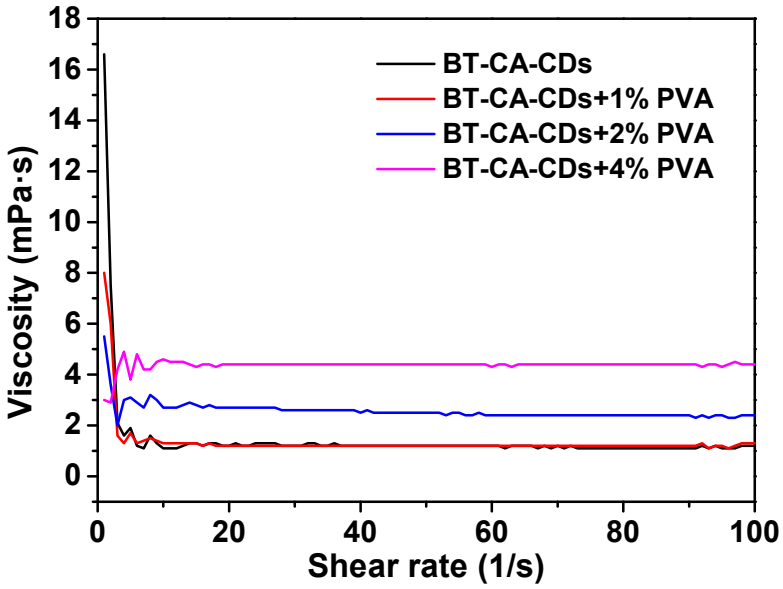

Figure S10. Viscosity of BT-CA-CDs solutions containing different concentrations of PVA (0, 1, 2 and 4 wt%). Higher PVA content leads to increased system viscosity.

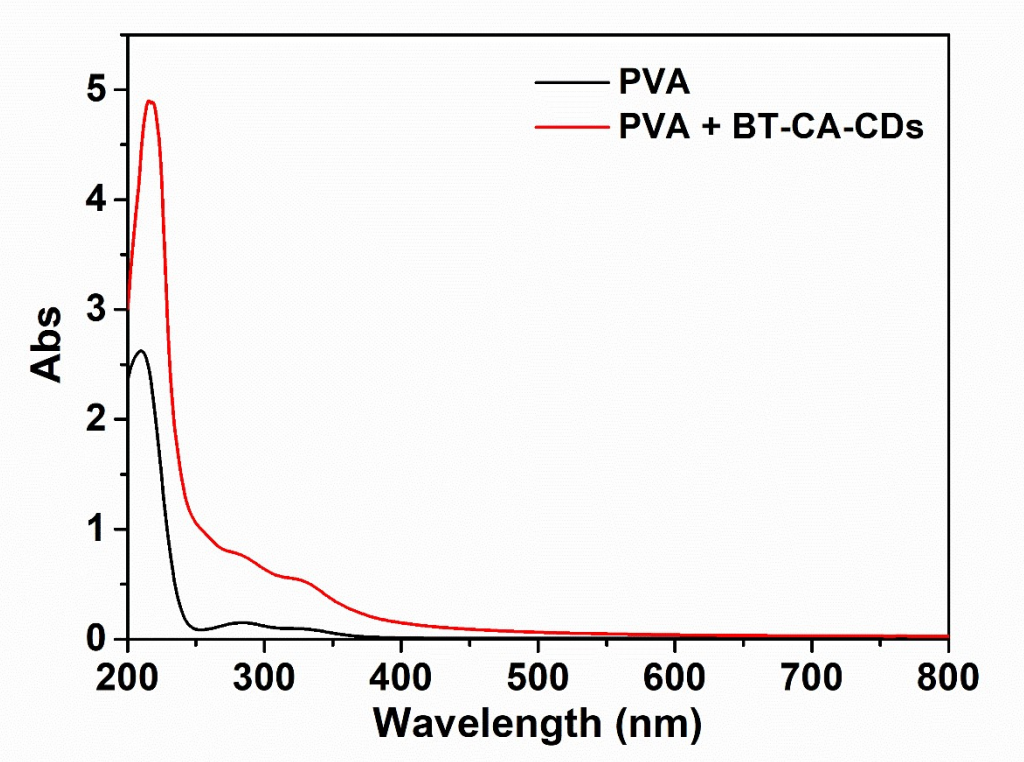

Figure S11. UV–vis absorption spectra of pure PVA and PVA + BT-CA-CDs composite (200–800 nm). The PVA + BT-CA-CDs composite exhibits significantly stronger UV absorption than pure PVA across the 200–400 nm range, demonstrating enhanced ultraviolet shielding capability.

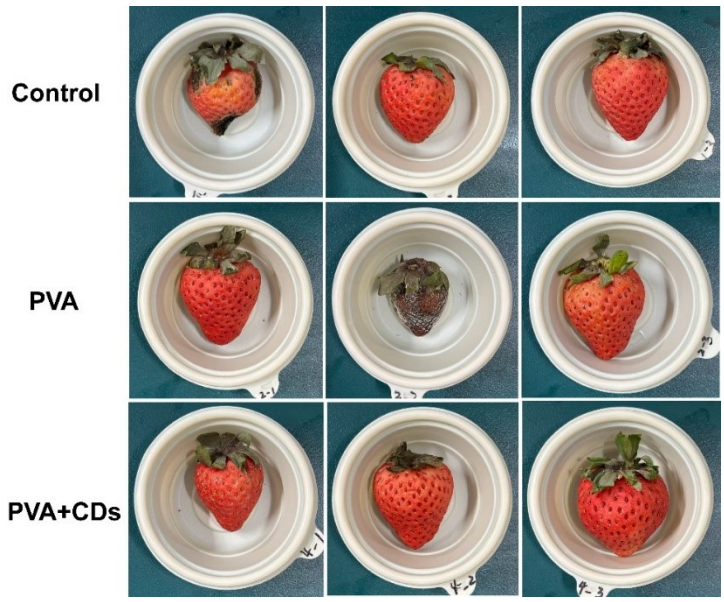

Figure S12. Digital images of strawberries on day 8 under different treatments (Control, PVA alone, and PVA+CDs). The PVA+CDs group shows the best preservation effect, characterized by fresh calyxes, vibrant fruit color, and no visible decay.

Table S1 Comparison of the preservation performance of the proposed method with recently reported active packaging and coating systems for strawberries.

Packaging system	Application method	Storage period (d)	Decay rate (%)	Weight loss (%)	Firmness retention (%)	References
CDs/PVA	Dip coating	6	0%	NA	NA	[1]
CDs/PVA/CMC	Packaging film	10	0%	NA	NA	[2]
SSPS-CQDs	Dip coating	5	0%	NA	NA	[3]
CDs/Gel	Dip coating	10	NA	~30%	~40%	[4]
MCQDs/PVA/CNC	Packaging film	8	<30%	38.0-40.2%	NA	[5]
Trp-CDs/CS/TA	Coating	≥5	NA	NA	NA	[6]
R-CDs/Gelatin	Dip coating	8	4.17%	~29.63%	~70%	[7]
CG-CDs	Packaging film	>8	0%	NA	NA	[8]
CDs/pectin	Packaging film	5	0%	~10%	NA	[9]
PVA+BT-CA-CDs	**Dip coating**	**6**	**0%**	**<20%**	**>70%**	**This work**

Referrences

1. M. Alas, G. Dogan, M. S. Yalcin, S. Ozdemir and R. Genç, *Acs Omega*, 2022, **7**, 29967-29983.
2. M. X. Hou, B. H. Xia, R. Y. Qu, J. L. Dong, T. Li, S. B. Wang, Y. Wang and W. F. Dong, *Int. J. Biol. Macromol.*, 2024, **273**, 132939.
3. Y. L. Xie, X. D. Geng, X. J. Zheng, J. Liu and K. Y. Tang, *Int. J. Biol. Macromol.*, 2025, **329**, 147893.
4. P. Y. Wang, M. N. Hu, H. M. Miao, M. H. Zan, Q. N. You and L. Li, *Food Chem.*, 2026, **507**, 148245.
5. X. J. Ma, X. Y. Su, F. Wang, W. L. Song, D. N. Li, J. N. Li and F. Qiao, *Food Packag. Shelf Life*, 2025, **52**, 101663.
6. L. L. Zhang, X. Gao, Y. M. Feng, Y. H. Yan, H. L. Zhu, S. P. Liu, Y. Yu and B. Yu, *ACS Appl. Mater. Interfaces*, 2023, **15**, 44097-44108.

7. B. Y. Guo, G. Liu, W. H. Ye, Z. Q. Xu, W. Li, J. L. Zhuang, X. J. Zhang, L. S. Wang, B. F. Lei, C. F. Hu, Y. L. Liu and H. W. Dong, *Food Hydrocolloids*, 2024, **147**, 109327.
8. N. T. Tran, T. N. Le, L. Nguyen, G. T. Nguyen and T. N. Ly, *RSC Adv.*, 2025, **15**, 50089-50102.
9. B. W. Shen, Z. X. Yan, T. F. Yang, L. Y. Zhu, Y. X. Wang and L. Jiang, *J. Food Eng.*, 2024, **364**, 111800.